Supplementary Information (SI) for Green Chemistry.
This journal is © The Royal Society of Chemistry 2026

Supporting information

Plastic waste boosted plasma-assisted ammonia synthesis process from N_2 and H_2O

Hangtian Hu,[1] Wenping Li,[1]* Hui Zheng,[1] Zheng Li,[1] Aiguo Wang,[1] Zhangxin Chen,[2] and Jinguang Hu[1]*

[1] Department of Chemical and Petroleum Engineering, University of Calgary, 2500 University Drive, NW, Calgary, Alberta T2N 1N4, Canada

[2] Eastern Institute of Technology, Ningbo, Zhejiang, 315200, China

E-mail: wenping.li@ucalgary.ca ; jinguang.hu@ucalgary.ca

The calculation of specific energy input (SEI, kJ L^{-1}) and energy efficiency (EE, mg/kWh) was shown below, where P_{total} is the input power (The input power used in this work refers to the applied plasma generator power, rather than the directly measured discharge power), Q is the total gas flow, and $C_{NH_3}$is the concentration of ammonia generated in the plasma process.

$$SEI = \frac{P_{total}}{Q}$$

$$EE_{NH_3} = \frac{C_{NH_3}}{SEI}$$

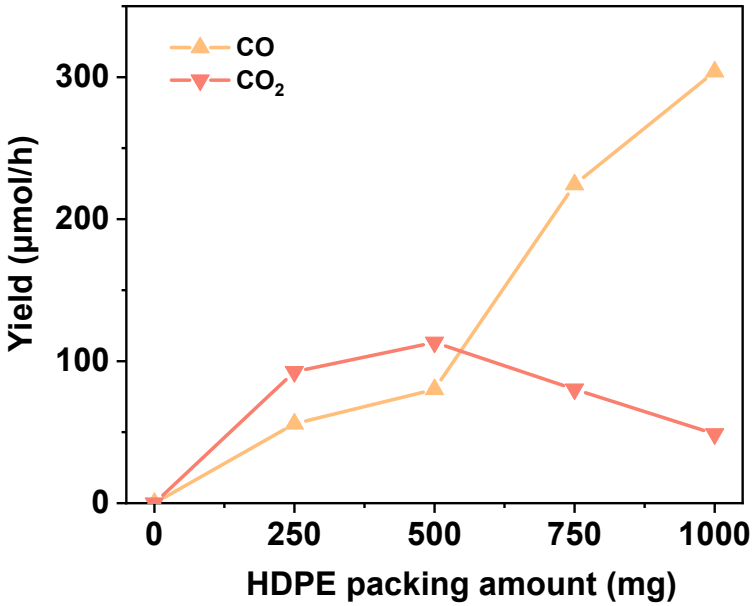

Fig. S1 Effect of HDPE packing amount on CO and CO_2 yields (feeding gas: N_2 + H_2O; flow rate: 10 SCCM; 2.64 mol% H_2O; input power: 40 W).

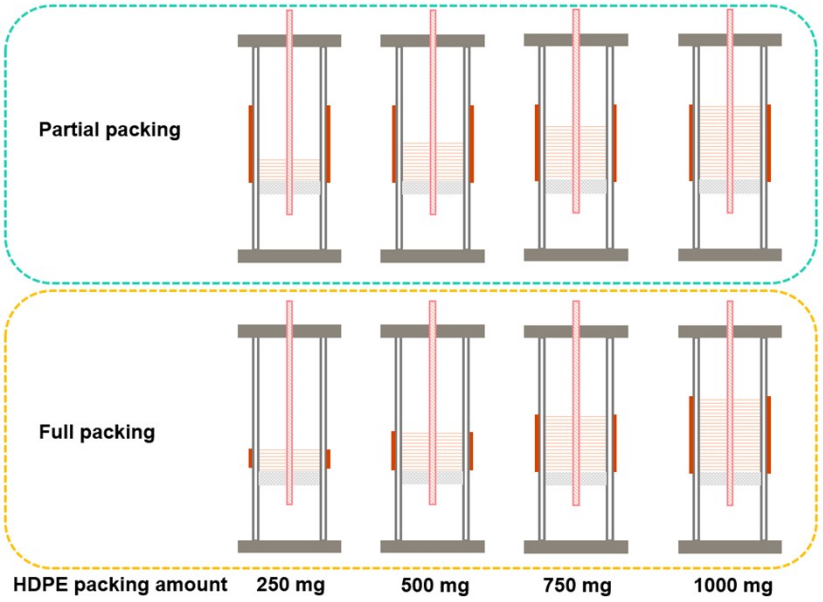

Fig. S2 Comparison of partial and full packing reactors at different HDPE packing amount.

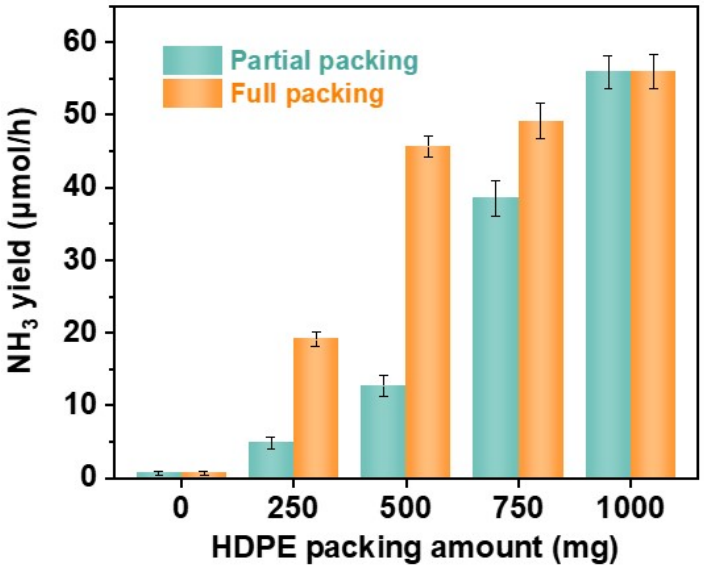

Fig. S3 Comparison of NH_3 yields for full and partial packing reactors at different HDPE packing amount (full packing; feeding gas: N_2 + H_2O; flow rate: 10 SCCM; 2.64 mol% H_2O; input power: 40 W).

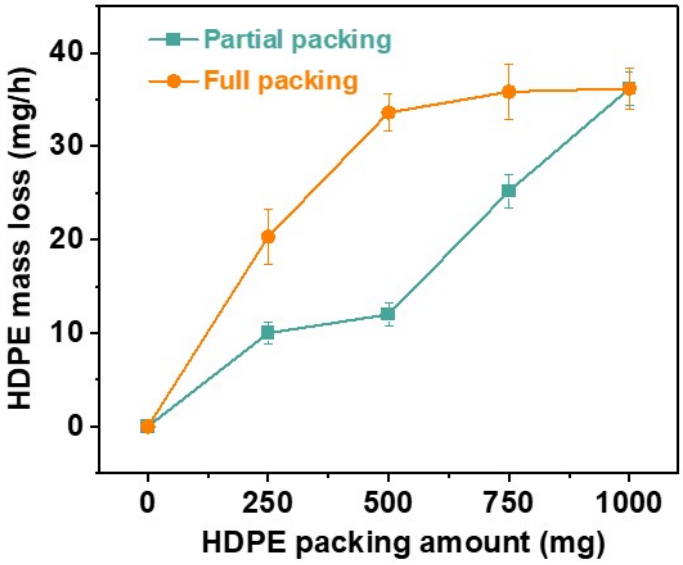

Fig. S4 Comparison of HDPE amount loss for full and partial packing reactors at different HDPE packing amount (full packing; feeding gas: N_2 + H_2O; flow rate: 10 SCCM; 2.64 mol% H_2O; input power: 40 W).

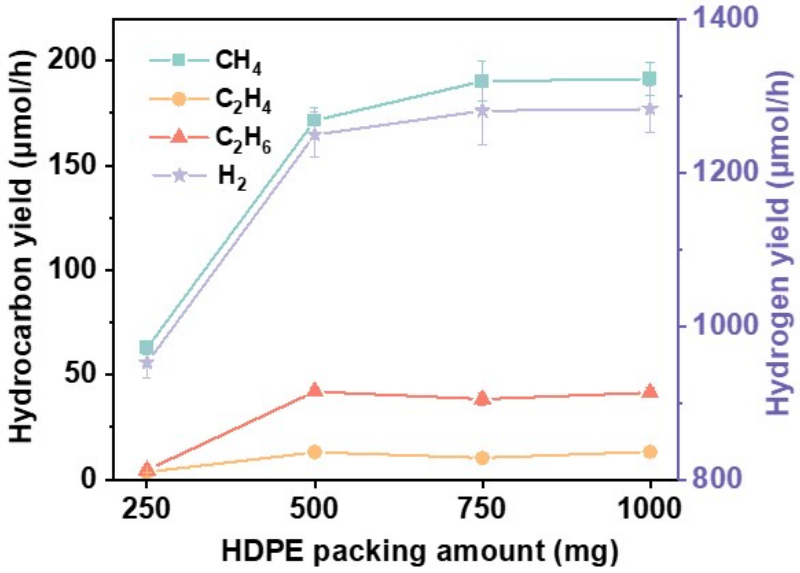

Fig. S5 Effect of HDPE packing amount on gaseous product yields (full packing; feeding gas: N_2 + H_2O; flow rate: 10 SCCM; 2.64 mol% H_2O; input power: 40 W).

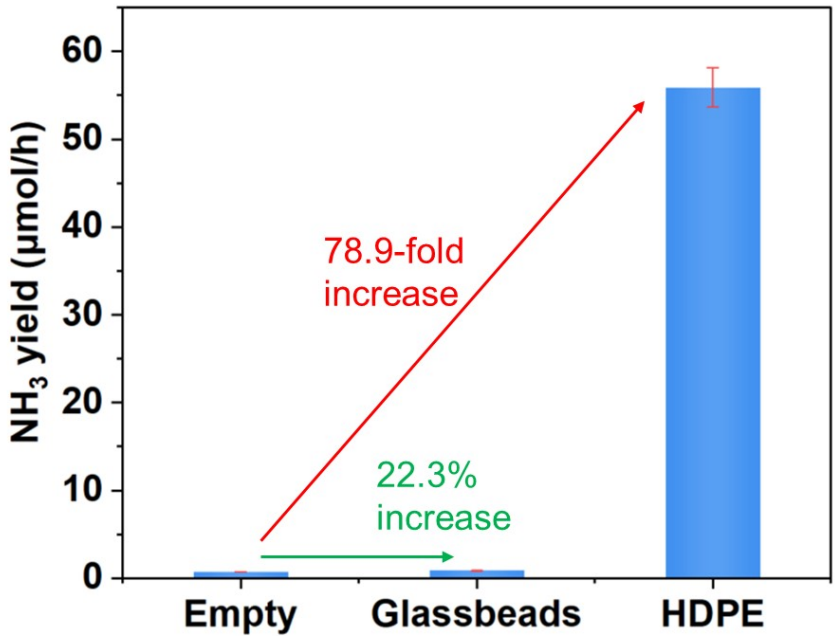

Fig. S6 Comparison of NH_3 yield over empty, glass bead-packed, and HDPE-packed DBD reactors. Reaction condition: full packing; feeding gas: N_2 + H_2O; flow rate: 10 SCCM; HDPE packing amount: 1000 mg; 2.64 mol% H_2O; input power: 40 W.

It should be noted that the introduction of HDPE packing may modify the discharge characteristics of the DBD reactor, including local electric field distribution and energy dissipation behavior. Because direct electrical diagnostics were not available in the present work, the observed enhancement is discussed as a combined result of discharge modification and changes in the reaction environment.

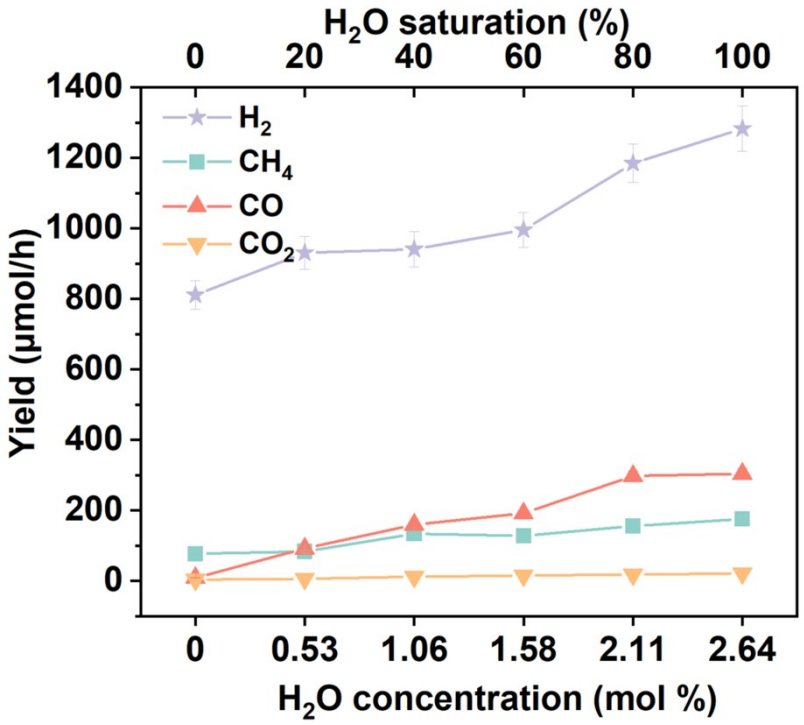

Fig. S7 Effect of H_2O concentration on gaseous product yields (full packing; feeding gas: N_2; flow rate: 10 SCCM; HDPE packing amount: 1000 mg; input power: 40 W).

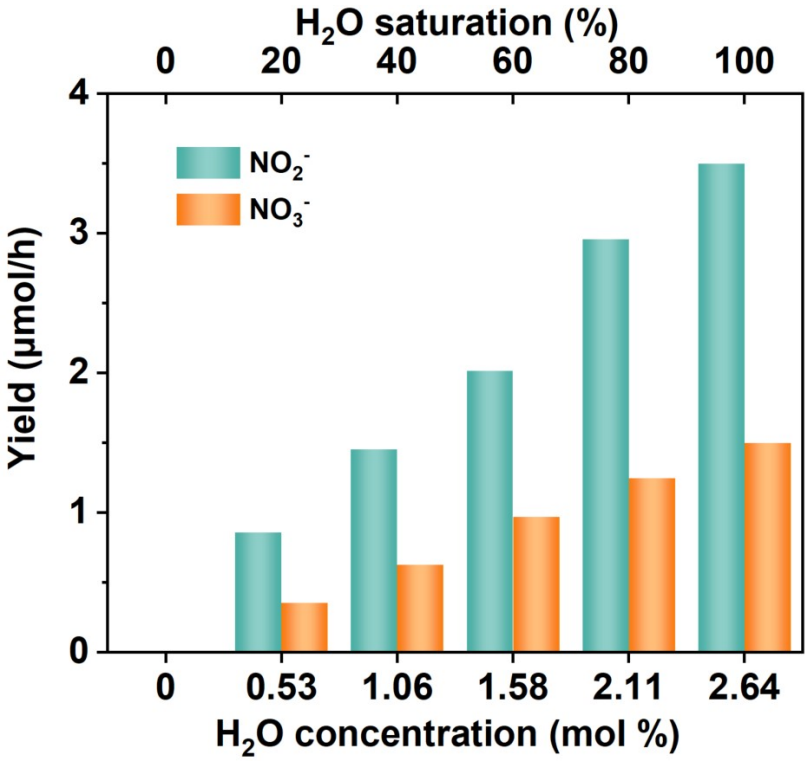

Fig. S8 Comparison of NO_2^- and NO_3^- yields at different H_2O concentrations in the feed gas. (full packing; feeding gas: N_2; flow rate: 10 SCCM; HDPE packing amount: 1000 mg; input power: 40 W).

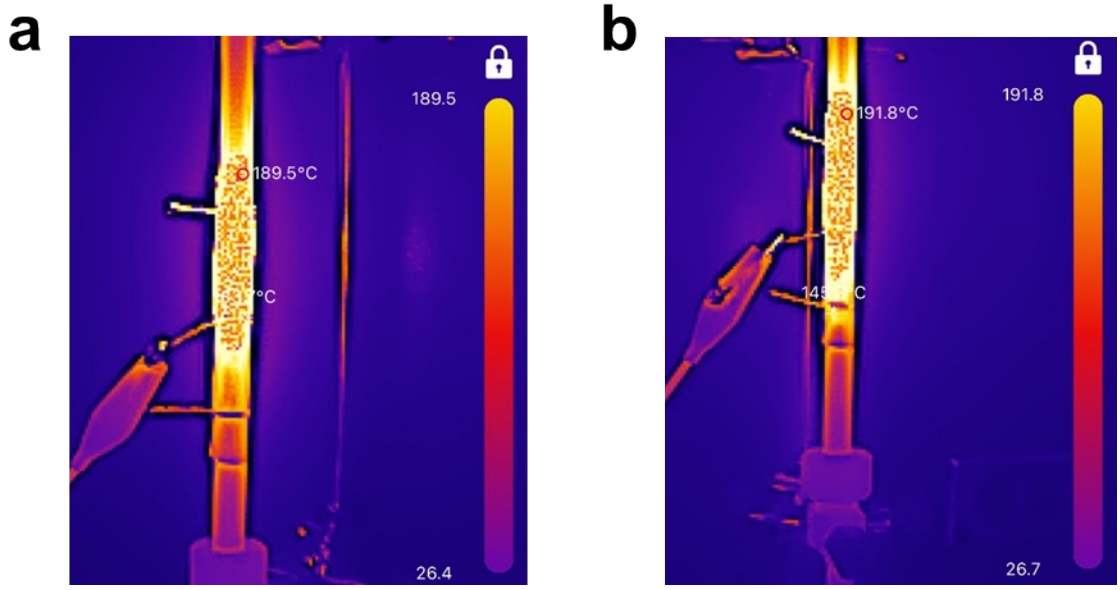

Fig. S9 Infrared thermal images of the reactor under identical reaction conditions: (a) empty tube and (b) HDPE-packed tube (feeding gas: N_2; flow rate: 10 SCCM; input power: 40 W).

Regarding temperature, the reactor temperature was monitored externally during operation using an infrared thermal camera (TOPDON TC002C). Repeated measurements showed that, when the applied input power was fixed at 40 W, the measured outer-wall temperature in the discharge region remained approximately 190 °C. Within the investigated range, no obvious difference in the outer-wall temperature was observed with varying H2O content or HDPE packing amount under the same applied input power. These results have been added to the revised supporting information.

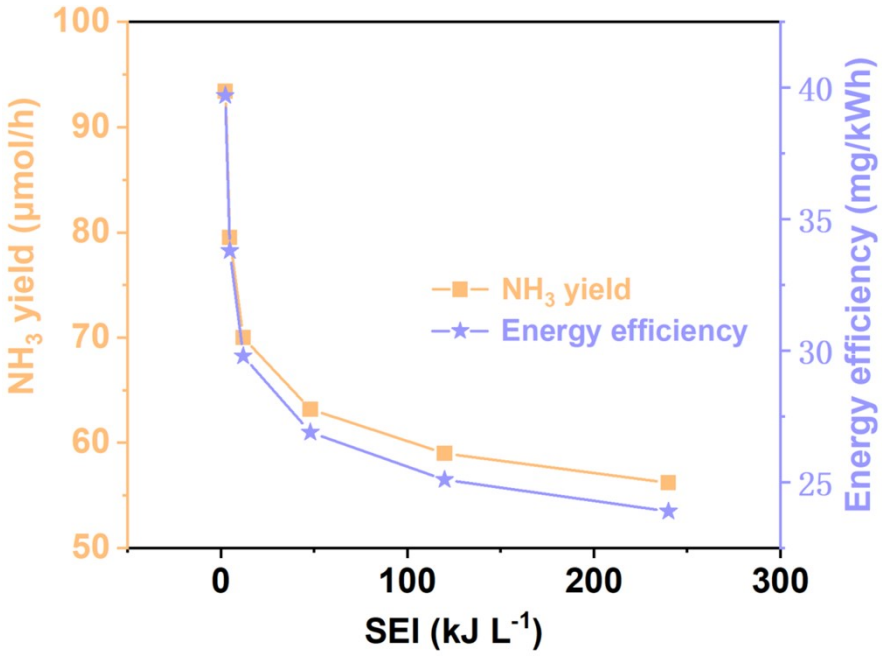

Fig. S10 Effect of SEI on NH_3 yield and energy efficiency (full packing; feeding gas: N_2 + H_2O; input power: 10 SCCM; 2.64 mol% H_2O; HDPE packing mass: 1000 mg; flow rate increased from 10 to 1000 sccm).

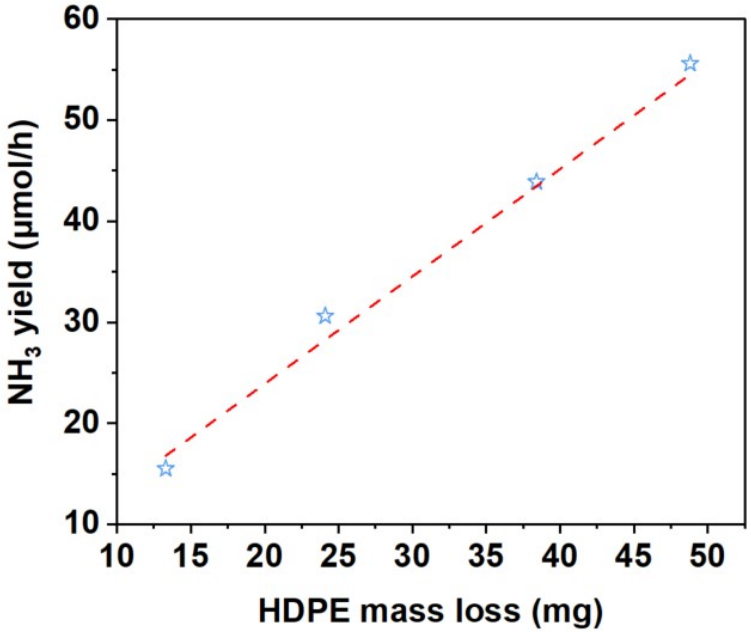

Fig. S11 Relationship between NH_3 yield and HDPE mass loss. Reaction condition: full packing; feeding gas: N_2 + H_2O; flow rate: 10 SCCM; HDPE packing amount: 1000 mg; 2.64 mol% H_2O; input power: 40 W.

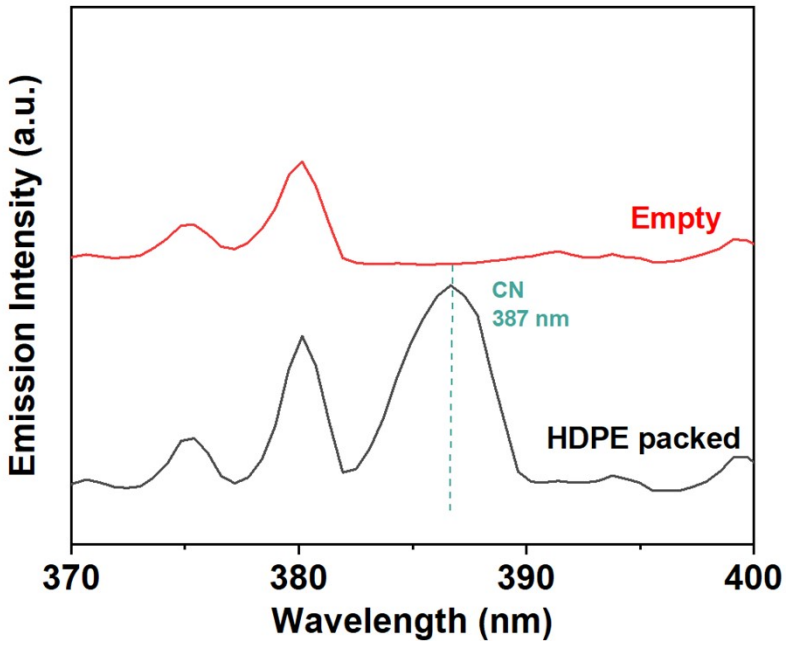

Fig. S12 Comparison of N_2 activation and optical emission spectrum for N_2-H_2O plasma between a full packing HDPE (1000 mg) reactor and an empty reactor (370-400 nm).

Table. S1 Repeatability analysis of NH_3 yield for different reaction conditions

	NH_3 yield					RSD
Ar/W	0.00	0.00	0.00	0.00	0.00	0
Ar/P	0.00	0.00	0.00	0.00	0.00	0
N_2/W	0.069	0.070	0.069	0.072	0.070	1.75%
N_2/P	31.11	37.39	35.21	34.52	36.12	6.77%
N_2/W/P	53.91	55.96	57.23	53.75	59.00	4.02%

Table S2. Comparative summary of this work and representative literature reports on NH_3 production rate and energy efficiency across electrified NH_3 synthesis systems.

Plasma N_2 reduction						
Plasma type	Hydrogen source	Gas feed	Catalyst	NH_3 yield (mg h^{-1})	Specific energy consumption (kWh kg^{-1})	Ref
DBD	H_2O vapor	N_2	Ru/MgO	3.49 - 4.52	6383-15459	[1]
DBD	H_2O vapor	N_2	γ-Al_2O_3	0.073	131062	[2]
DBD	H_2O vapor	N_2	5-rGO-TiO_2	21.40	758.9	[3]
Plasma electrolytic system	H_2O electrolyte	N_2	N/A	0.44	2270	[4]
DBD	H_2O droplet	N_2	N/A	0.18	125000	[5]
DBD/UV	H_2O	N_2	N/A	0.034	N/A	[6]
Plasma jet	H_2O vapor	N_2	N/A	0.064	1552–1928	[7]
DBD	H_2O vapor	N_2	N/A	0.44	118482	This
DBD	H_2O vapor	N_2	HDPE	1.65	30864	work

Direct electrocatalytic N_2 reduction					
Electrolyte	Gas feed	Catalyst	NH_3 yield	Specific energy consumption (kWh kg^{-1})	Ref
0.1 M Na_2SO_4	N_2	Janus-Ni/MoO_2	5.87×10^{-3} mg h^{-1} cm^{-2}	16.1	[8]
acidic H_2SO_4 (pH=2)	N_2	WO_xN_γ/WO_3	19.6×10^{-3} mg h^{-1} cm^{-2}	16.3	[9]
0.1 M Na_2SO_4	N_2	Ru-VOH	0.115 mg h^{-1} mg_{cat}^{-1}	13.1	[10]

0.1 M HCl	N_2	ZnTe	19.9×10^{-3} mg h^{-1} mg_{cat}^{-1}	138.7	[11]
0.1 M Na_2SO_4	N_2	CNMS	71.1×10^{-3} mg h^{-1} mg_{cat}^{-1}	38.9	[12]
10 M LiCl	N_2	SAB/C	58.1×10^{-3} mg h^{-1} cm^{-2}	10.2	[13]

Li-mediated N_2 reduction

Electrolyte	Gas feed	Key design	NH_3 FE (%)	Specific energy consumption (kWh kg^{-1})	Ref
1.0 M $LiBF_4$, THF	N_2, 1 bar	Phenol as proton shuttle and buffer	72	34.4	[14]
1 M $LiBF_4$, THF, 0.25 vol% EtOH	N_2	$LiBF_4$ salt screening	61	39.7	[15]
THF/LiTFSI + TTE antisolvent	N_2, 20 bar	Localized high-concentration electrolyte	73.6	N/A	[16]
2 M lithium difluoro(oxalato)borate	N_2	Enhanced Li-ion diffusion	98	24.6	[17]
High- concentration imide-based Li salt electrolyte	N_2	Compact ionic layering, interfacial assembly	Near 100	30.4	[18]

Table. S3 Carbon balance calculation in an hour process. Reaction condition: full packing; feeding gas: N_2 + H_2O; flow rate: 10 SCCM; HDPE packing amount: 1000 mg; 2.64 mol% H_2O; input power: 40 W.

Mass of carbon (mg)						
HDPE carbon loss	Gaseous byproducts				Liquid byproducts	Error (%)
	CH_4	C_2H_6	CO	CO_2		
34.40	2.17	1.12	3.94	0.72	24.45	5.52

Table. S4 Hydrogen balance calculation in an hour process. Reaction condition: full packing; feeding gas: N_2 + H_2O; flow rate: 10 SCCM; HDPE packing amount: 1000 mg; 2.64 mol% H_2O; input power: 40 W.

Mass of hydrogen (mg)							
HDPE hydrogen loss	H_2O dissociation	Gaseous byproducts			Liquid byproducts	NH_3	Error (%)
		H_2	CH_4	C_2H_6			
7.70	0.78	2.60	0.73	0.28	4.08	0.17	8.18

References:

1. T. Zhang, R. Zhou, S. Zhang, R. Zhou, J. Ding, F. Li, J. Hong, L. Dou, T. Shao, A. B. Murphy, K. Ostrikov and P. J. Cullen, *Energy Environ. Mater.*, 2022, **6**, e12344.
2. J. Feng, P. Ning, K. Li, X. Sun, C. Wang, L. Jia and M. Fan, *ACS Sustain. Chem. Eng.*, 2023, **11**, 804-814.
3. S. Song, F. Wang, X. Sun, Y. Chen, J. Liu, Y. Shi, P. Ning, Y. Ma and K. Li, *ACS Catal.*, 2025, **15**, 17603-17613.
4. S. G. Ryan Hawtof, Evan Guarr, Cheyan Xu, R. Mohan Sankaran, Julie Nicole Renner, *Sci. Adv.*, 2019, **5**, eaat5778.
5. J. R. Toth, N. H. Abuyazid, D. J. Lacks, J. N. Renner and R. M. Sankaran, *ACS Sustain. Chem. Eng.*, 2020, **8**, 14845-14854.
6. T. Sakakura, S. Uemura, M. Hino, S. Kiyomatsu, Y. Takatsuji, R. Yamasaki, M. Morimoto and T. Haruyama, *Green Chem.*, 2018, **20**, 627-633.
7. Y. Gorbanev, E. Vervloessem, A. Nikiforov and A. Bogaerts, *ACS Sustain. Chem. Eng.*, 2020, **8**, 2996-3004.
8. L. Li, Y. Li, K. Li, W. Zou, H. Li, Y. Li, L. Li, Q. Zhang, C. Zhang, X. Zhang, D. Tian and L. Jiang, *ACS Nano*, 2025, **19**, 1080-1089.
9. Z. Zhang, C. Kondratowicz, J. Smith, P. Kucheryavy, J. Ouyang, Y. Xu, E. Desmet, S. Kurdziel, E. Tang, M. Adeleke, A. D. Lele, J. M. Martirez, M. Chi, Y. Ju and H. He, *ACS Energy Lett.*, 2025, **10**, 3349-3358.
10. Y. Sun, X. Li, Z. Wang, L. Jiang, B. Mei, W. Fan, J. Wang, J. Zhu and J. M. Lee, *J. Am. Chem. Soc.*, 2024, **146**, 7752-7762.
11. S. J. Mane, N. B. Joseph, R. Kumari, A. Narayan and A. J. Bhattacharyya, *ACS Mater. Au.*, 2024, **4**, 582-591.
12. R. Liu, T. Guo, H. Fei, Z. Wu, D. Wang and F. Liu, *Adv. Sci. (Weinh)*, 2022, **9**, e2103583.
13. M. Wang, S. Liu, H. Ji, T. Yang, T. Qian and C. Yan, *Nat. Commun.*, 2021, **12**, 3198.
14. X. Fu, A. Xu, J. B. Pedersen, S. Li, R. Sazinas, Y. Zhou, S. Z. Andersen, M. Saccoccio, N. H. Deissler, J. B. V. Mygind, J. Kibsgaard, P. C. K. Vesborg, J. K. Norskov and I. Chorkendorff, *Nat. Commun.*, 2024, **15**, 2417.

15. X. Fu, S. Li, N. H. Deissler, J. B. V. Mygind, J. Kibsgaard and I. Chorkendorff, *ACS Energy Lett.*, 2024, **9**, 3790-3795.
16. H. Yun, C. Lim, M. Kwon, D. Lee, Y. Yun, D. H. Seo and K. Yong, *Adv. Mater.*, 2024, **36**, e2408280.
17. H. L. Qiang Zhang, Peiping Yu, Pengyu Liu, Ning Sun, Yiyan Wang, Chunlai Tu, Yiping Liu, Yan Wang, Xinyang Yue, Linlin Ma, Wen Wen, Jinyang Xu, Zhaofeng Liang, Jingyuan Ma, Fei Song, Zheng Liang, Hao Sun, Daishun Ling, Hongyan Liang, Feng Liu, Yongfeng Hu, Tao Cheng, Jun Li, *Science*, 2026, **391**, 724-729.
18. H. L. Du, M. Chatti, R. Y. Hodgetts, P. V. Cherepanov, C. K. Nguyen, K. Matuszek, D. R. MacFarlane and A. N. Simonov, *Nature*, 2022, **609**, 722-727.
19. M. Guláš, C. S. Cojocaru, F. Le Normand and S. Farhat, *Plasma Chem. Plasma Process.*, 2007, **28**, 123-146.
20. H. M. Nguyen, F. Gorky, S. Guthrie and M. L. Carreon, *Catal. Today*, 2023, **418**, 114141.